Lectures - Thursday, June 22, afternoon

L5

X-RAY IMAGING

Jürgen Härtwig

ESRF, Grenoble, France

L6

SYNCHROTRON TOPOGRAPHY AS AN UNIQUE TOOL FOR INVESTIGATION OF VARIOUS PHYSICAL PHENOMENA

Petra Pernot and José Baruchel

ESRF, Grenoble, France

Introduction

Synchrotron radiation topography is used for the investigation of many types of domains, phase coexistence, or field related defects in magnetic and ferroelectric single crystals. The origin of the contrast either resides in i) the variation of electrostrictive, magnetostrictive, or space charge related, distortions, or, ii) by taking advantage of the coherence of the beam, from a contrast mechanism associated with the variation of the structure factor phase between neighbouring domains.

Ferroelectric crystals: the example of KTP

We are concerned with ferroelectric 180° domain walls, that behave as af twin boundary that separates regions of opposite polarity.

The aim of this study was to understand the structure of domain walls in $KTiOPO_4$ (KTP) crystals and to extract from coherent X-ray Bragg diffraction imaging a very elusive information about atomic arrangements at domain walls. We used for this a combined Bragg and Fresnel imaging technique that takes advantage of the coherence of the synchrotron X-ray beam, and was succesfuly used for LNO [1] and KTA [2] crystals. The domain walls were introduced by the method of periodic poling. This means that the ferroelectric polarization (and the crystal structure) is inverted in the created neighbouring domains. X-ray diffraction by these, neighbouring "up" and "down" domains differ both through the amplitude and phase of the structure factors. However, by far the largest contribution to the contrast between the domains is produced by the difference in phase, which is principally structural in origin. The value of this "phase jump", calculated from the crystal structure depends very sensitively on how the crystal structures of the domains are matched or linked across the domain wall. From crystallographic principles, five possible domain-matching schemes have been suggested for KTP crystals. Each of these matching schemes introduces a different phase shift in Bragg diffraction from inverted domains. Therefore, by measuring the actual value of and comparing it with values calculated from these models, atomic-level information about the domain wall can be inferred.

Fig. 1 shows reflection topographs of a 9 mm period KTP sample using the 004 reflection. The contrast simulations are presented on the right side of the each experimental image. The simulations were performed for = -38.6°, expected if the P(1) atom acts as a pivot for the twinning. Fig. 2 shows the set of monochromatic section topographs in transmission of a periodically poled KTP sample with 24.7 mm period as a function of the sample-to-detector distance, using the 140 reflection. The simulated images correspond to = 180°. The model of twinning resulting from our investigation is shown in Fig. 3. The translation 1/2(**a**+**b***)* relates equivalent atoms in adjacent domains in addition to the shift in the *c*-direction [3].

Magnetic crystals: -Fe_2O_3 and MnP

We will give two examples of magnetic phase transitions, where real time X-ray topography provides physical information that is not available otherwise.

Spin-reorientation Morin transition in hematite

Hematite (-Fe_2O_3) is a weak ferromagnet at room temperature. It undergoes a spin-reorientation transition (the Morin transition, T_M 260K) towards a low temperature antiferromagnetic state. Previous investigations indirectly suggested that the boundaries that form during this transition are nearly parallel to the (111) plane. The present study was motivated by the possibility of using high energy X-ray *section* diffraction imaging, which allows the direct visualization of the boundaries along the depth of a thick sample. The Morin transition was therefore visualized by observing phase boundary movements under the influence of temperature and of a magnetic field, on white beam section topographs, with the FreLoN camera as detector. The sample was a high quality (111) platelet shaped crystal, 1.1 mm thick. Figure 4 shows the phase boundaries movement within the topographic images (corresponding to virtual slices of the sample), while remaining nearly parallel to (111). These images were recorded at a fixed temperature,

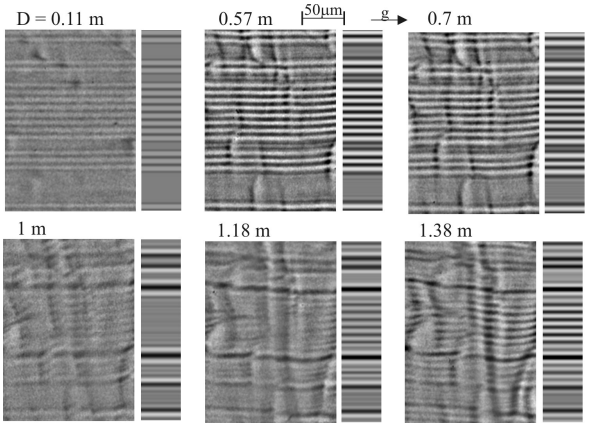

Fig. 1. White beam projection topographs (004) in reflection and their simulations as a function of the sample-to-detector distance.

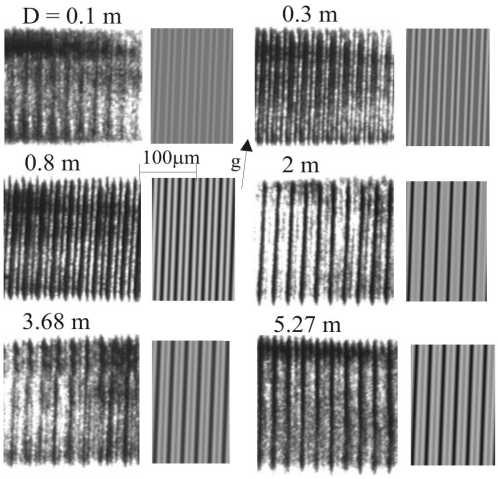

Fig. 2. Monochromatic section topographs (140) in transmission and their simulations.

within the antiferromagnetic phase (258 K) whereas increasing the magnetic field (60 mT, 180 mT and 235 mT in fig. 4) that favours the weak ferromagnetic phase. The nucleation of the weak ferromagnetic phase and pinning of interphase boundaries on defects located in the bulk of the crystal were observed. The observed behaviour patterns were explained in terms of the elastic and magnetostatic energies involved [4].

Fan to ferromagnetic transition in MnP

MnP can be produced as highly perfect single crystals. It exhibits a complex magnetic phase diagram, which easily allows alterations in the ratio between the various energy terms relevant for the phase coexistence. The ferromagnetic - fan coexistence was found [5] to display a thick, interface between the two magnetic phases (figure 5). Complementary investigations were performed on a (001) MnP crystal, under a magnetic field applied along the **b** direction, at T 48 K, in order to understand this unusual phase boundary.

It was observed that the ferromagnetic-fan interface includes bulk transition regions, elongated along **a**, and thick enough along the **b** direction (in the 10^{-4} m range) to produce a substantial contribution to diffraction. The Bragg

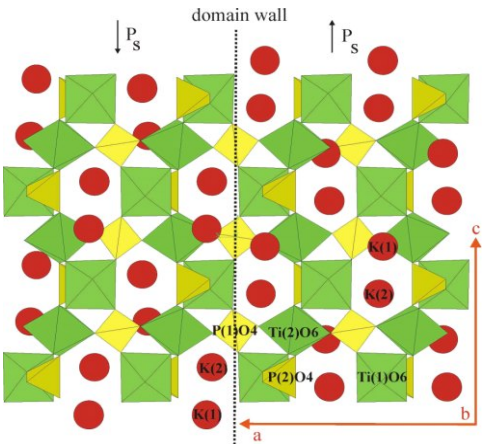

Fig. 3. Schematic view of a domain wall (dotted line) passing through the atom P(1).

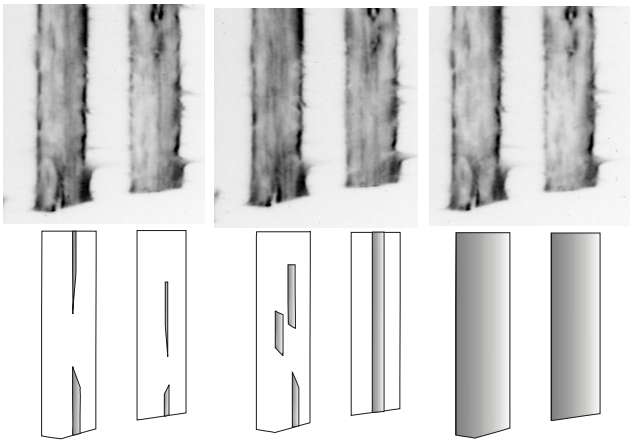

Fig. 4. Evolution of wo section topographs recorded during the Morin transition as a function of the magnetic field. The width of a given section corresponds to 0.35 mm. The schematic representation of the section topographs shows the progression of the weak ferromagnetic phase, (shaded regions).

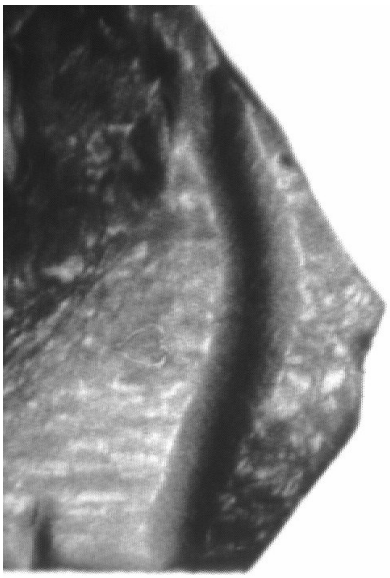

Fig. 5. Monochromatic topograph recorded during the ferro to fan transition, which shows the thick phase boundary (a is vertical and b horizontal; scale bar: 1 mm).

condition changes continuously across these regions. This configuration, which involves magnetic charge distribution, is in sharp distinction with the usual two-dimensional character of magnetic walls and phase boundaries. A model of the thick interface comprising a set of intermediate magnetic states that only occur during the ferromagnetic-fan phase coexistence, was proposed to explain the observations [6]. The very unusual fact is that, if this model applies, this thick interface is not expected to imply a substantial increase in elastic energy, because locally each magnetic state exhibits its spontaneous distortion, ideally leading to no long-range stress.

1. Rejmánková-Pernot P, Cloetens P, Baruchel J, Guigay J-P and Moretti P 1998 *Phys. Rev. Lett*. **81** 3435.
2. Rejmánková-Pernot P, Thomas P A, Cloetens P, Lorut F, Baruchel J, Hu Z W, Urenski P and Rosenman G 2000 *J. Appl. Cryst*. **33** 1149.
3. Pernot-Rejmánková P, Thomas P A, Cloetens P, Lyford T and Baruchel J 2003 *J. Phys.:Condens. Matter* **15** 1613.
4. Schetinkin S.A., Wheeler E., Kvardakov V.V., Schlenker M.and Baruchel J. 2003 *J. Phys. D: Appl. Phys* 36, A118-A121.
5. Medrano C., Pernot E., Espeso J., Boller E., Lorut F.and Baruchel J. 2001 *Journal of Magnetism and Magnetic Materials* 226-230, 623-625.
6. Baruchel J., Medrano C.and Schlenker M 2005 *J. Phys. D: Appl. Phys* 38, A67-A72.

L7

FAST MICROTOMOGRAPHY

Marco Di Michiel

ESRF, Grenoble, France

L8

EVOLUTION OF THE SPONTANEOUS LATERAL COMPOSITION MODULATION IN InAs/AlAs SUPERLATTICES ON InP

O. Caha[1], V. Holý[1,2], K. E. Bassler[3]

[1]Institute of condensed matter physics, Masaryk University, Brno, Czech Republic
[2]Department of electronic structure, Charles University, Praha, Czech republic
[3]Department of physics, University of Houston, Houston, USA
caha@physics.muni.cz

During growth of short-period superlattices, spontaneous lateral composition modulation can occur leading to a quasiperiodic modulation of the thicknesses of individual layers; resulting one-dimensional nanostructures (quantum wires) have potential applications in optoelectronics [1]. Theoretical description of the modulation process is based on two different models. If there is a high density of monolayer steps on the vicinal surface (the crystallographic miscut angle is larger than approx. 1^{O}), a step-bunching instability occurs [2], but if the density of the the monolayer steps is low, a self-organized growth of two-dimensional or three-dimensional islands takes place. The latter process occurs, if the reduction of the strain energy due to an elastic relaxation of internal stresses in the islands outweighs the corresponding increase of the surface energy (morphological Asaro-Tiller-Grinfeld (ATG) instability [3]).

The dependence of the lateral composition modulation on the number of layers was investigated using grazing incidence X-ray diffraction. The serie of four samples of InAs/AlAs superlattices grown by molecular beam epitaxy (MBE) on an InP(001) substrate was studied; the substrate was prepared without any nominal miscut. The samples have 2, 5, 10 and 20 superlattice periods; the InAs and AlAs thicknesses were nominally 1.9 monolayers in all samples. For all samples, we have measured the intensity distribution of the grazing-incidence 400 and 040 diffraction in the $q_x q_y$ plane of the reciprocal space, i.e. parallel to the sample surface. The x-ray measurements have been carried out at the beamline ID01 of the European Synchrotron Radiation Facility (ESRF, Grenoble).

From the experiment follows that the modulation amplitude increases with the number of layers, the lateral modulation period $\langle L \rangle$ = (267 ± 15) Å remains constant during the growth, while the width of the lateral satellites decreases with N as $N^{-0.2}$ [4].

From this behavior it follows that the first stages of the spontaneous modulation of the average chemical composition of a short-period superlattice cannot be explained as a result of the bunching of monolayer steps at the interfaces. Most likely, this behavior can be ascribed to the ATG instability, in which the critical wavelength of the surface corrugation, L_{crit} depends on the stress in the growing layer, elastic constants and its surface energy. The evolution of the surface morphology of multilayers has been studied only in a linearized approach so far [5]. From this approach, an unlimited growth of the modulation amplitude follows, which does not correspond to the experimentally

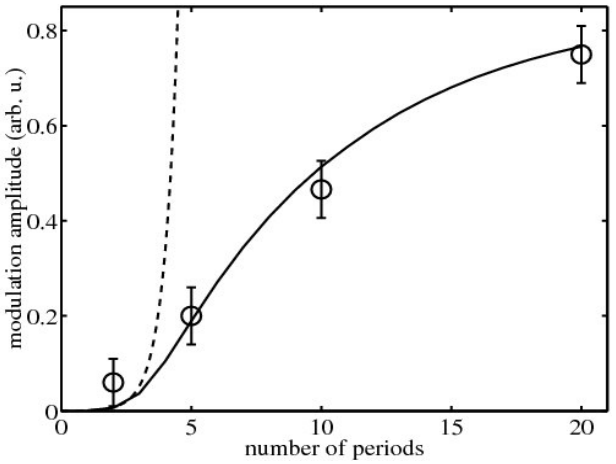

Figure 1. The dependence of the modulation amplitude on the number of superlattice periods. The circles with error bars are the experimental points obtained from the X-ray data, the full line represents the simulations. The dashed line is the evolution of the modulation amplitude calculated in the linearized approach [5].

observed stabilization of the modulation amplitude during the growth.

We have simulated a full nonlinear time evolution equation of the spontaneous lateral modulation and we have obtained the critical wavelength L_{crit} = 300 Å. The particular values of diffusion rate have only weak influence on the resulting interface morphology. We have also found that the nonlinear dependence of the strain energy on the layer thickness (wetting effect) has a crucial influence on the resulting interface morphology. The parameters of this nonlinear dependence were determined from the fit of the experimental data with the simulation and these values were compared with the atomistic calculation [6]. The resulting experimental and theoretical dependence of the modulation amplitude on the number of superlattice periods is plotted in Fig. 1.

1. A. G. Norman, S. P. Ahrenkiel, C. Ballif, H. R. Moutinho, M. M. Al-Jassim, A. Mascarenhas, D. M. Follstaedt, S. R. Lee, J. L. Reno, E. D. Jones, R. D. Twesten, and J. Mirecki-Millunchick, *Mater. Res. Soc. Symp. Proc.* **583**, 297 (2000).
2. L. Bai, J. Tersoff, and F. Liu, *Phys. Rev. Lett.* **92**, 225503 (2004).
3. R. J. Asaro and W. A. Tiller, Metall. Trans. **3**, 1789 (1972); M. A. Grinfeld, *Sov. Phys. Dokl.* **31**, 831 (1986).
4. O. Caha, P. Mikulík, J. Novák, V. Holý, S. C. Moss, A. Norman, A. Mascrenhas, J. L. Reno, and B. Krause, *Phys. Rev. B* **72,** 035313 (2005).
5. Z.-F. Huang, R. C. Desai, *Phys. Rev. B* **67**, 075416 (2003).
6. O. Caha, V. Holý, and K. E. Bassler, *Phys. Rev. Lett.* **96**, 136102 (2006).

Lectures - Friday, June 23, morning

L9

X-RAY SCATTERING ON SURFACES AND NANOSTRUCTURES

Hartmut Metzger

ESRF, Grenoble, France

L10

X-RAY SCATTERING FROM SELF-ORGANIZED SEMICONDUCTOR NANOSTRUCTURES - OUR RESULTS AND HOPES FOR FUTURE

Václav Holý

Department of Electronic Structures, Faculty of Mathematics and Physics, Charles University Prague, Czech Republic

The determination of shapes, elastic deformations, and local chemical composition of semiconductor nanostructures (quantum wires and dots) by x-ray scattering is a challenging task requiring to use very intense energy-tunable x-ray sources. The shapes of nanostructures can be studied by small-angle X-ray scattering (the GISAXS method), while the elastic strains and local chemical composition can be determined by diffraction (coplanar X-ray diffraction or grazing-incidence diffraction). Recently, new methods appeared making use of the possibility of energy tuning of the synchrotron radiation, namely anomalous x-ray diffraction close to the absorption edge and diffraction anomalous fine structure method (DAFS) measuring the energy dependence of the diffracted intensity just above the absorption edge. These methods can give direct information on the chemical composition of nanostructures. In the talk, the scattering methods used for nanostructures are briefly summarized, illustrated by experimental results obtained at ESRF.